Research Square

Preprints are preliminary reports that have not undergone peer review.
They should not be considered conclusive, used to inform clinical practice,
or referenced by the media as validated information.

# Excellent Photocatalytic Degradation of Indigo Dye using Low Cost Chemical Route Grown Highly Luminescent SnO2 Decorated Polystyrene Nanocomposites

**Jyoti Bala Kaundal**
Jiwaji University

**R.K Tiwari**
Jiwaji University Faculty of Physical Sciences

**Y C Goswami** ( y_goswami@yahoo.com )
ITM University https://orcid.org/0000-0002-7499-1711

**Research Article**

**Keywords:** Metal oxides, SnO2, Photoluminescence, Polymer nanocomposites, Chemical route, Polystyrene nanocomposites, recyclable expended polystyrene waste

**Posted Date:** February 19th, 2021

**DOI:** https://doi.org/10.21203/rs.3.rs-213335/v1

**License:** This work is licensed under a Creative Commons Attribution 4.0 International License.
Read Full License

**Excellent Photocatalytic degradation of Indigo dye using low cost chemical route grown highly luminescent $SnO_2$ decorated Polystyrene nanocomposites**

Jyoti Bala Kaundal, R.K Tiwari* and Y C Goswami,

Nano research lab, Department of Physics, School of Sciences, ITM University, Gwalior

*SoS in Physics, Jiwaji University Gwalior

**Email**: ycgoswami@gmail.com

**Abstract**

Irrational use of dye is a challenge for our environment specifically for clean water. Highly luminescent $SnO_2$ decorated Polystyrene nanocomposites developed as an effective solution for it. The low cost chemical synthesis of highly luminescent tin oxide decorated Polystyrene ($SnO_2$-PS) polymer nanocomposites using recyclable expended polystyrene waste has been reported. Sol gel grown tin oxide nanoparticles, thoroughly dissolved in dissolved in toluene were used with recyclable expended polystyrene waste. The composites were grown either on glass substrates or developed as flexible self sustaining layers and characterized by optical, structural & morphological characterizations. X ray diffractograms of $SnO_2$-PS polymer nanocomposites exhibit crystalline behavior with tetragonal structure of $SnO_2$. Accumulation of $SnO_2$ particles on the surface with increasing concentration, in the form of spherical structures is observed in AFM micrographs. Hollow vertical chain like growth is also observed. Absorption edge shift towards higher wavelength results in decrease in band gap with increasing concentration. The Photoluminescence (PL) spectra for higher $SnO_2$ shows a significant peak peaks in visible spectra at about 425 nm. $SnO_2$ decorated Polystyrene nanocomposites synthesized using recyclable expended polystyrene waste opens a new scope in flexible optoelectronic applications with visible region photoluminescence.

**Keywords:** Metal oxides; $SnO_2$, Photoluminescence, Polymer nanocomposites, Chemical route; Polystyrene nanocomposites, recyclable expended polystyrene waste

**Introduction**

Modernization caused an irrational use of dyes, and resulted in severe environment thereats. As a result, degradation of dyes have now become an urgent area of research [1]. Recently Nano photocatalysts showed a new promising way to address this challange. Despite of their improved properties, the small size of the nano composites also come up with issues like difficulty in their separation, lack of process for reuse, and also a possible risks to ecosystems by the potential release of the nanoparticles into the environment [2,3]. An efficient approach to overcome the above drawbacks is to immobilize the nanosized particles into a host material of larger size namely in a polymer nanocomposite. Polystyrene (PS) has shown its best candidature for such nanocomposites. Bekri-abbes et al. [4] has reported converting polystyrene waste into cation exchange resin. Achilias et al. [5] has reported sulfonation recycling to convert polymer waste into useful material. Maharana

et al. [6] also reported the gaseous and liquid form of recycled polystyrene depending upon temperature and reaction catalyst. Solubility and stability of polystyrene wastage in recycling process studied by Garcia et al. [7]. Instead of recycling the PS, development of Semiconductor PZ nano composits for various application is also realized recently. In this regard, Chae et al,[8] reported decrease in tensile strength of polystyrene composites on increasing concentration of ZnO Nanoparticles PS. Soon Ma et al. [9] also reported resistivity of ZnO/PS Nanocomposite decreases as the amount of ZnO increases in the composites. In exploring other properties Zhong et al. [10] reported about change in magnetization property of $fe_3O_4$ in $Fe_3O_4$/PS nanocomposites. G. Nenna et al. [11] exhibited that the optical properties of ZnO/PS and showed that theses nanocomposites can improve the light extraction in Organic Light-Emitting Diode. Ali et al. [12] has prepared Nanocomposite films of $Fe_3O_4$/PS having good thermal stability and supermagnetic behavior. It is used in chemical sensor and supercapacitor. Qianqian Ding et al. [13] reported that PS/Cu Nanocomposites with enhanced Raman scattering performance. Kassaee et al, and polystyrene [14, 15] have been studied that polystyrene as an organic material for the synthesis of composites with inorganic materials like PS-$fe_3O_4$, PS-$MnO_2$, PS-ZnO, PS-$ZrO_2$, many other polystyrene based compounds are given in Polystyrene: synthesis, characteristics, and applications. In other applications Deborah Ruziwa et al.[16] reported that sulphonated waste polystyrene to remove the heavy metal ions like $Zn^{2+}$ and $Pb^{+2}$, However to the best of our knowledge very less on PS/SnO2 nanocomposites have been reported. SnO2 is an important n-type wide band gap (3.6 eV at 300 K) semiconductor [17]. It owes significant electrical, optical, and electrochemical properties and have potential applications as functional blocks in future nano devices [18-29]. Geovania C. de Assis et al. [30] has been reported PS/ $SnO_2$ nanocomposites for photocatalytic degradation of dyes. Yong-Qiang Liuet al. [31] have reported their work on Micro-patterned PS/$SnO_2$ films by using microparticles of $SnO_2$. In the present work first time we have reported sol gel grown highly luminescent Polystyrene -$SnO_2$ nanocomposites using recyclable expanded polystyrene waste and Photocatalytic degradation of Indigo dye using this composite.

**Experimental details**

$SnO_2$ decorated Polystyrene nanocomposites were synthesized using recyclable expended polysterene waste. Starting materials were AR grade Stannous chloride ($SnCl_2$) Toluene, Acetone, obtained by Ranbaxy and used without further purification. Thoroughly cleaned soda lime glass was used as substrates for the synthesis. The whole process of synthesis has been divided in the following steps:

1. Preparation of PS solution
2. Preparation of $SnO_2$ Nanoparticles
3. Formation of PS-$SnO_2$ Nanocomposites films on glass and self-sustained layers
4. Formation of PS-$SnO_2$ films.

**Step 1. Preparation of PS solution**

Thermocol waste (a form of PS) which is used as packaging material, collected and thoroughly cleaned with distilled water and then sonicated to remove dust, crushed into small pieces and finally dried for 12 hours at room temperature. The pieces were added in 60 ml toluene and stirred magnetically for 10 minutes. The Thermocol get dissolved and resulted in transparent solution.

**Step 2. Preparation of $SnO_2$ Nanoparticles and their solutions**

$SnO_2$ Nanoparticles were obtained using sol gel route using the method already been reported [23]. The different weights of obtained $SnO_2$ particles (A1: 1g, A2: 3g and A3: 5g) were added in 20 ml of acetone and stirred continuously for one an hour after which it was kept in ultasonicator at $30^0$C for another hour.

**Step3. Formation of PS-$SnO_2$ nanocomposites films on glass and self-substrate**

$SnO_2$ dissolved in Acetone (A1, A2, A3), were added in 20 ml of PS solution separately and stirred for another 10 minutes finally spread on glass substrates to get films using doctors blade method.

**Step4. Formation of PS-$SnO_2$ films.**

For film deposition, thoroughly cleaned Soda glass slides having dimension 10mm x10mm were used as substrate. PS-$SnO_2$ solution of various ratios were dropped on these substrates and spread evenly using doctor blade method and then dried at room temperature. After several hours the films are self-etched from the glass substrate.

**Experimental setup and procedure**

Photocatalytic experiments were performed in a photo reactor using our own designed setup. The set up has a provision for continuous stirring and 4 LED light source of 10 Watt each. for It's a wooden case magnetic stir inside it, maintained at 25±1ºC by circulating the coolant through fan. The reactor was painted by black color to prevent other light. For irradiation experiments, the desired concentrations of Indigo solution were prepared. The reaction suspensions were formed by addition various concentration of PS $SnO_2$ polymer nanocomposites (films) in 20mL solution of indigo carmine dye. The suspensions were stirred in the dark thoroughly for 30min to achieve the adsorption/desorption equilibrium.

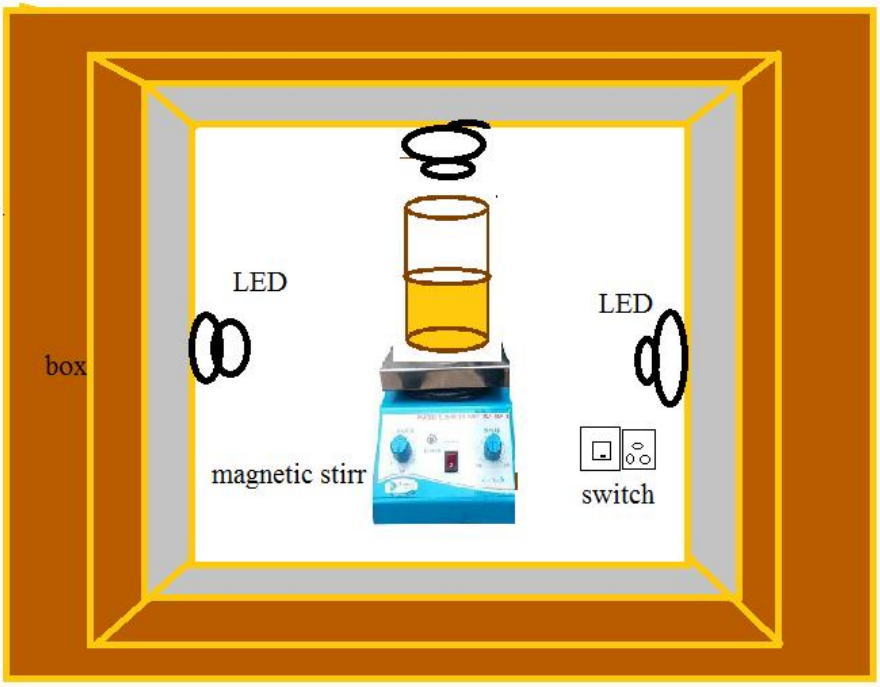


**Fig.1. schematic diagram of Photocatalytic reactor Photocatalytic activity**

The photocatalytic activities of the samples were evaluated by photodegradation of the Indigo carmine under a simulated sunlight from a 40Watt LED bulbs at room temperature. The 4ppm solution of dye solution is prepared with 40 mg of Dye dissolved in 100ml of distilled water. The reaction suspensions formed by 20Mg of various concentration of PS- $SnO_2$ flexible films and 20mL of each indigo carmine dye solution .the film suspensions solutions were stirred in the dark for 30min to achieve the adsorption/desorption equilibrium.

After 30min, a small amount of the solution was withdrawn for analysis of the indigo carmine concentration after filter. The photodegradation of the indigo carmine solution was investigated by measuring its absorbance by the UV-Vis spectrophotometer (Perkin Elmer Lambda-25) at the maximum absorption around $\lambda$max = 6000nm. A good linear relationship between the concentration and absorbance at low concentration is presented according to Lambert-Beer's law:

$$\text{Percentage degradation} = \frac{(C0-Ct)*100)}{C0}$$

where $C0$ is the initial concentration of indigo carmine solution, $A0$ means the initial absorbance, $Ct$ is the concentration. The samples were removed from the dye after30 min. form the photocatalytic experiment solution. These samples were recycled again for further analysis. The photocatalytic experiments were performed using aqueous solutions of Indigo dye at different catalyst dosages .

**Characterization**

All the samples were analyzed by structural, morphological and optical characterizations. X-ray diffractograms were obtained for the angle in the range 10° to 60° using Bruker D8 Advanced XRD with using Cu k target. AFM micrographs were obtained by using Tapping mode IUAC Indore. PL, UV-Vis spectra were carried by Perkin Elmer Lambda-25 and Photoluminescence (PL) spectra obtained by Perkin Elmer LS-55.

**Results and discussion**

PS-$SnO_2$ nancomposites grown on glass or self sustained films were analyzed using optical, structural and morphological characterizations.

**Structural Studies**

X-ray diffraction pattern of PS, PS/$SnO_2$ flexible self-sustained films grown on glass substrate are shown in Fig. 2 (a) and 2(b).

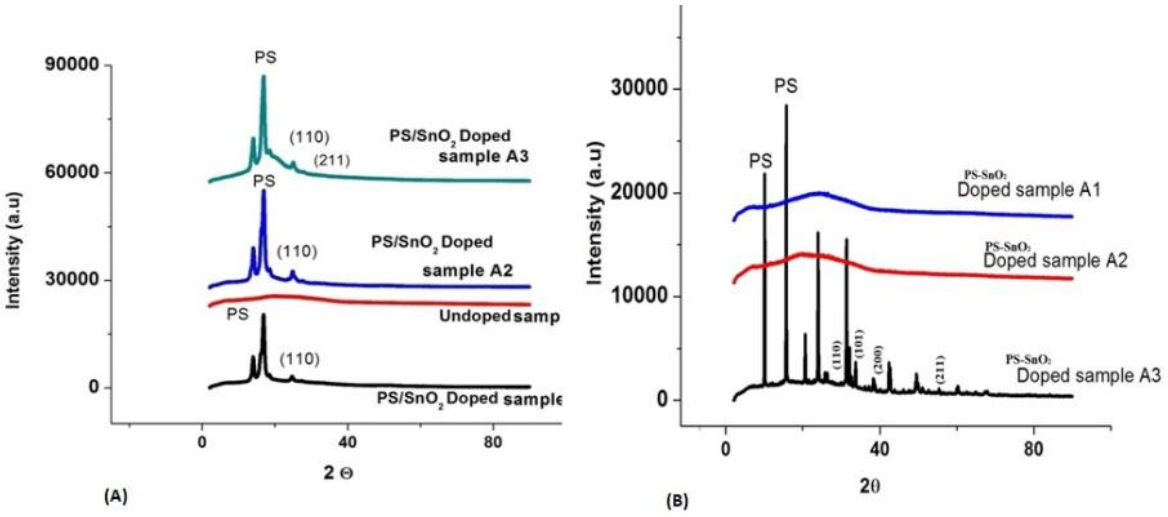


**Fig.2. X ray diffractograms for (a) flexible self sustained films (b) on glass substrate with various $SnO_2$ concentrations (A) Undoped A0 (B) A1:1g PS/ $SnO_2$ (C)A2:3g PS/$SnO_2$ (D) A3: 5g PS/ $SnO_2$.**

In fig. 2(a), X- ray diffractograms for PS/ $Sn_2$ flexible self-sustained films with various $SnO_2$ concentrations are shown. No peak is observed in bare PS diffractogram shows amorphous behavior of Polystyrene, however with addition of increasing concentration of $SnO_2$ the sharp peaks of PS are observed at about or below 20 degrees, for various molar concentration of PS/$SnO_2$. (110) (211) of $SnO_2$ are observed and verified with JCPDS file (card No: 41-1445). X ray diffractograms for PS/ $SnO_2$ on glass substrate with various $SnO_2$ concentrations are shown in Fig 2(b). No peaks are observed in diffractograms for sample A1 and A2 indicates the amorphous nature however diffractogram for Sample A3 show (110), (101), (200), (211) planes for $SnO_2$ by verified with the JCPDS file (card No: 41-1445) which shows the presence of $SnO_2$ nanoparticles of tetragonal positions.

The average nano-crystallite size (D) was calculated using the Scherrer formula,

$$D = {}^{0.9\lambda}/_{\beta Cos\theta} \cdots\cdots\cdots [32]$$

Where λ is the X-ray wavelength, θ is the Bragg diffraction angle, and β is the FWHM of the XRD peak appearing at the diffraction angle θ. The crystalline sizes were estimated from the Scherer's relation and found to be about 14nm, 12nm and 5nm of sample A1, A2, A3 and $A_0$ is amorphous in nature. It indicates that increase in the doping concentration of PS, decreases the average crystalline size. The intensity of peaks increases as the concentration of nanoparticles increases in samples. Also the film of PS/$SnO_2$ on glass substrate shows amorphous nature at low amount of $SnO_2$ in PS. And average size of crystallite is 36.2nm in A3 sample. The WH plot, strain and intercept of crystallite shown in Fig3. According to WH plot the crystallite shows that the composite experienced compressive strain due to its slope is negative.

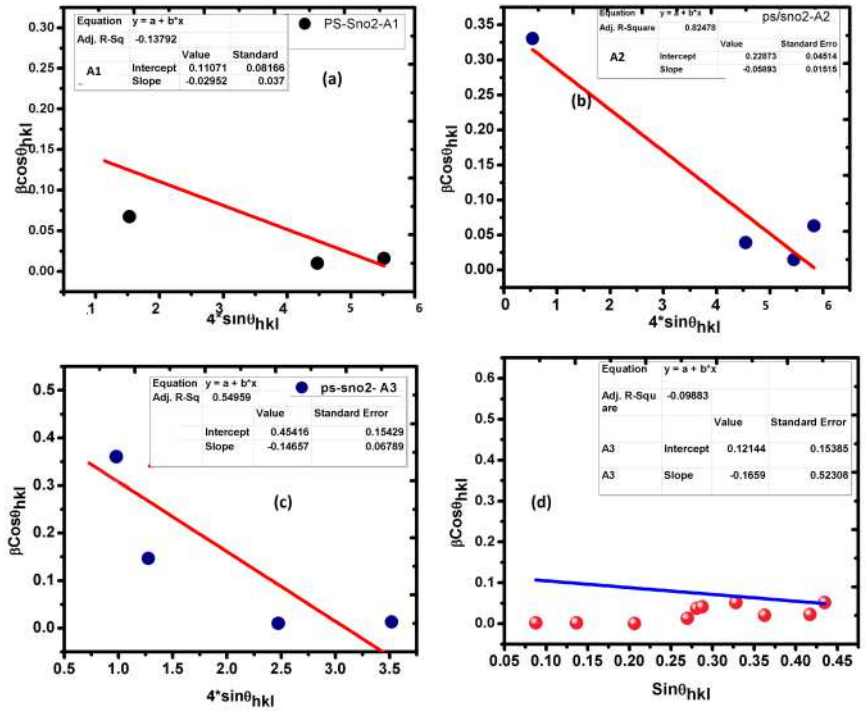


**Fig.3. W H plots of film on glass substrate (a), (b), (c). and in fig (d) WH plot of flexible film sample A3 with slope and intercept.**

**Table1.Particle size and strain calculation using Debeye- Scherrer formula and Williamson-Hall plot of Flexible and Glass substrate films of PS/$SnO_2$.**

| Debeye- Scherrer formula and Williamson-Hall plot. (Flexible) | | | | Debeye- Scherrer formula and Williamson-Hall plot(glass substrate film) | | | | |
|---|---|---|---|---|---|---|---|---|
| **Sample** | **FWHM** | **D Size** | **Intercept** | **Strain** | **Intercept** | **Strain** | **FWHM** | **Size** |
| **A0** | **Amorphous Nature** | | | | **Amorphous Nature ( A0,A1,A2)** | | | |
| **A1** | **0.0775** | **14.34** | **0.1107** | **-0.029** | **Amorphous Nature ( A0,A1,A2)** | | | |
| **A2** | **0.106** | **12.05** | **0.228** | **-0.0589** | **Amorphous Nature ( A0,A1,A2)** | | | |
| **A3** | **0.164** | **5.36** | **0.454** | **-0.146** | **.01244** | **-0.1659** | **0.07858** | **36.2nm** |

**Morphological studies**

Atomic force micrographs (AFM) of $SnO_2$/PS Nanocomposites (Sample A1, A2 and A3) are shown in Fig.4. Spherical structures arranged in a row are obtained in size of several nanometers. Hollow vertical growth may help in improving absorbing properties of the samples. The size of spherical structures increases as the concentration of $SnO_2$ nanoparticles increases in PS. Spherical structures aligned in regular manner like a chain. The roughness of spherical structures is increases as the concentration of $SnO_2$ decreases**.** Particle size and strain calculation using Debeye- Scherrer formula and Williamson-Hall plot and roughness calculation using AFM studies shown in Table2.

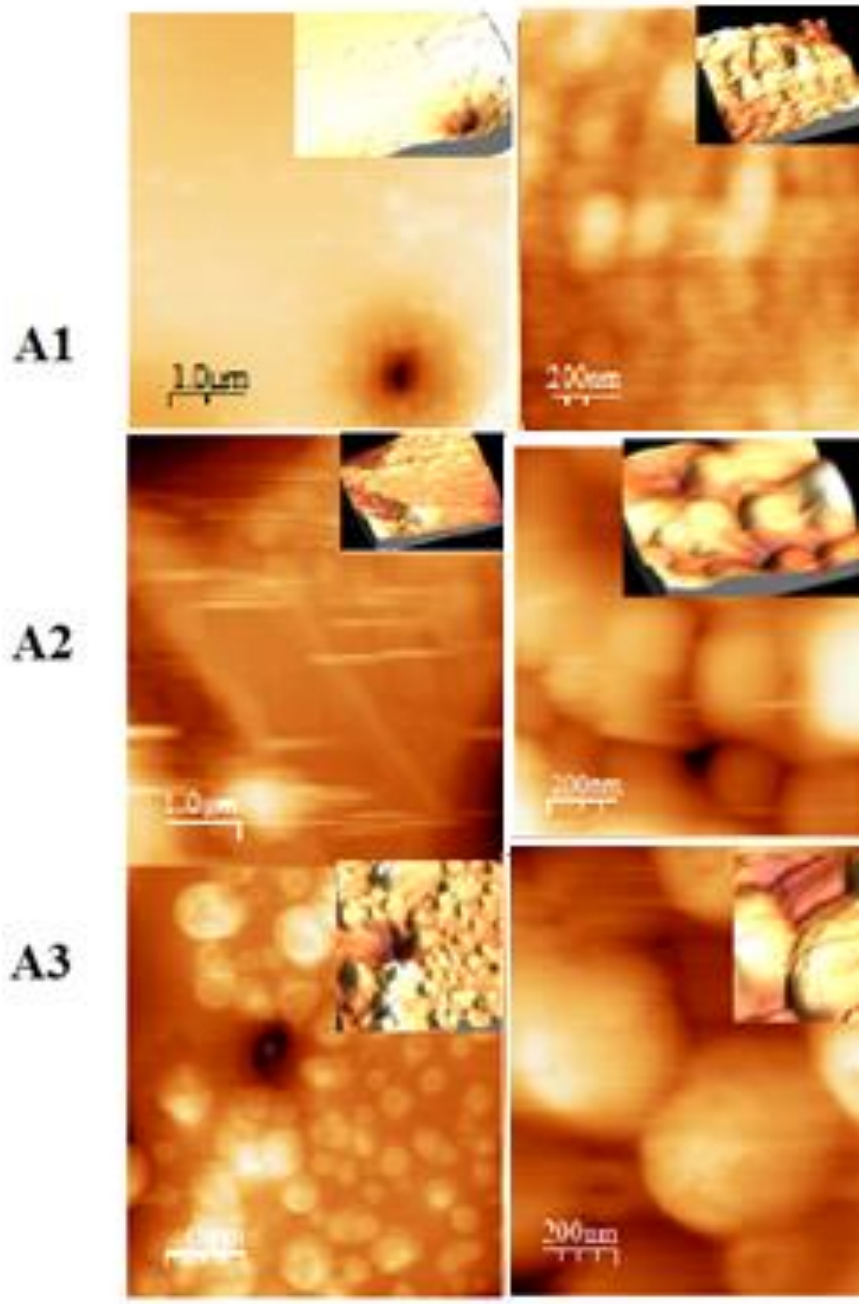


**Fig.4. Atomic force micrograph of $SnO_2$/PS Nanocomposites 2D view and 3D view of samples (a) A1-PS/ $SnO_2$ (b) A2-PS/ $SnO_2$ (c) A3-PS/ $SnO_2$.**

**Table2. Roughness calculation using AFM studies of flexible films.**

| **Roughness calculation using AFM studies** | | | | |
|---|---|---|---|---|
| **Scale** | **Rms Roughness(nm)** | **Average Roughness(nm)** | **Surface Skewness** | **Surface Kurtos** |
| **1.0µm** | **72.6571** | **53.3421** | **-0.7549** | **4.7191** |
| **1.0 µm** | **126.391** | **95.842** | **-0.5141** | **3.6176** |
| **1.0 µm** | **153.193** | **112.046** | **-0.715** | **4.4106** |

**FTIR**

FTIR spectral analysis was performed to confirm the chemical structure of all of the PS/ $SnO_2$composites. Figure 5 summarizes the FTIR spectra of the PS/ $SnO_2$ composites. Form the (Figure 5.) the spectrum shows the typical characteristic bands for Polystyrene at 2949, 3045, 1621 and 1498 cm−1, which correspond to the aliphatic C–H and –CH2 and the aromatic C=C stretching, respectively. Finally, four peaks in the region from 3000 to 3500 cm−1 correspond to aromatic C–H and =C–H stretching. Peaks obtained below 1000$cm^{-1}$ shows SnO2 nanoparticles present in film. The intensity of peaks increases as the concentrations of $SnO_2$ nanoparticles increase in polystyrene. Table2. Shows the molecular vibrations present in PS/$SnO_2$ composite. All the functional groups confirms that the PS/$SnO_2$ formation.

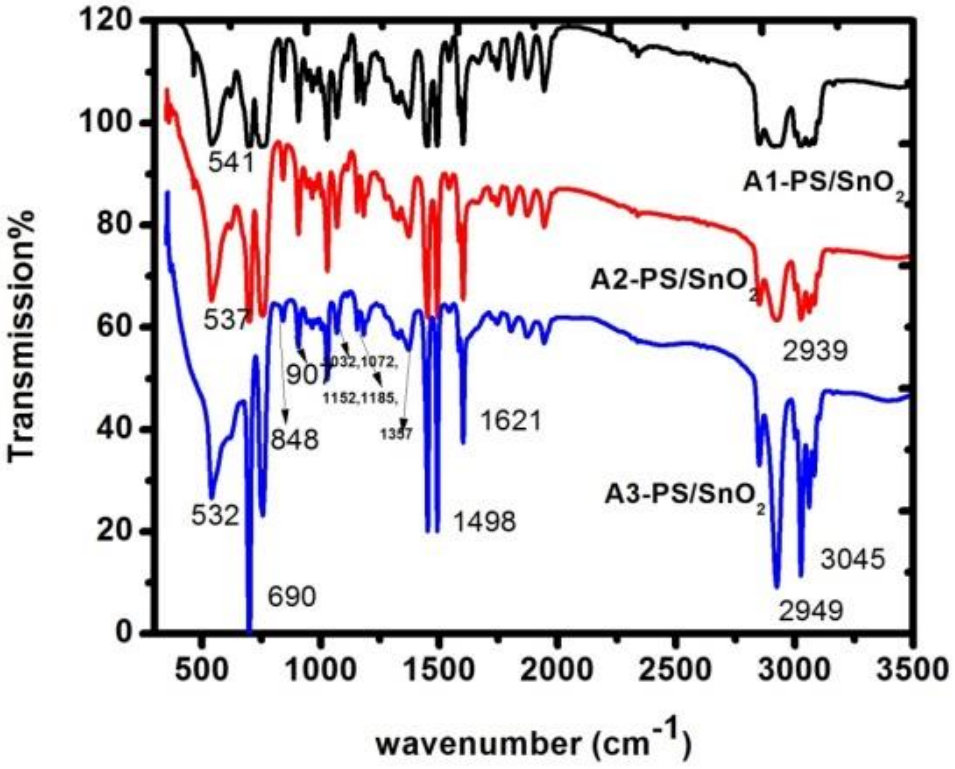


**Figure 5. FTIR spectra of (A) Undoped A0 (B) A1:1g PS/ $Sno_2$ (C) A2:3g PS/$Sno_2$ (D) A3: 5g PS/ $SnO_2$.**

**Table3. PS/$SnO_2$ IR-Spectrum Bands Wave numbers $cm^{-1}$ attributed stretching vibrations.**

| Stretching | A1 Wavenumber $cm^{-1}$ | A2 Wavenumber $cm^{-1}$ | A3 Wavenumber $cm^{-1}$ |
|---|---|---|---|
| Ar–H stretching | 2857,2949,3045 | 2837,2923,3081 | 2850,2917,3042 |
| C=C | 1621 | 1601 | 1608 |
| Ar- C-C | 1498-1357 | 1489-1377 | 1495-1377 |
| Ar-C-H | 848,907 | 841,908 | 848,908,973 |
| C-H | 690,742 | 709,755 | 696,762 |
| Sn | 532 | 537 | 550 |

**Optical Studies**

Absorption spectra of $SnO_2$ of different ratios were obtained shown in Fig. 6(a) . $SnO_2$ particles show good transmission in visible region, however overall absorption increases with increasing concentration of $SnO_2$ in PS. The $(\alpha h\nu)^2$ vs $h\nu$ plot were obtained and shown shown in Fig.6b. $SnO_2$ exhibits band gap about 3 eV suitable for optoelectronic applications. The band gap is decreases as the concentration of $SnO_2$ is increases. The results supports the AFM results. Photoluminescence spectra of $SnO_2$ Samples with concentration A1, A2 and A3 are shown in Fig6c. Samples exhibits

luminescence peak in 350 -450 nm region and very small peak at 850 nm. It may be due to transition between band deeply trapped holes in $SnO_2$ nanoparticles.

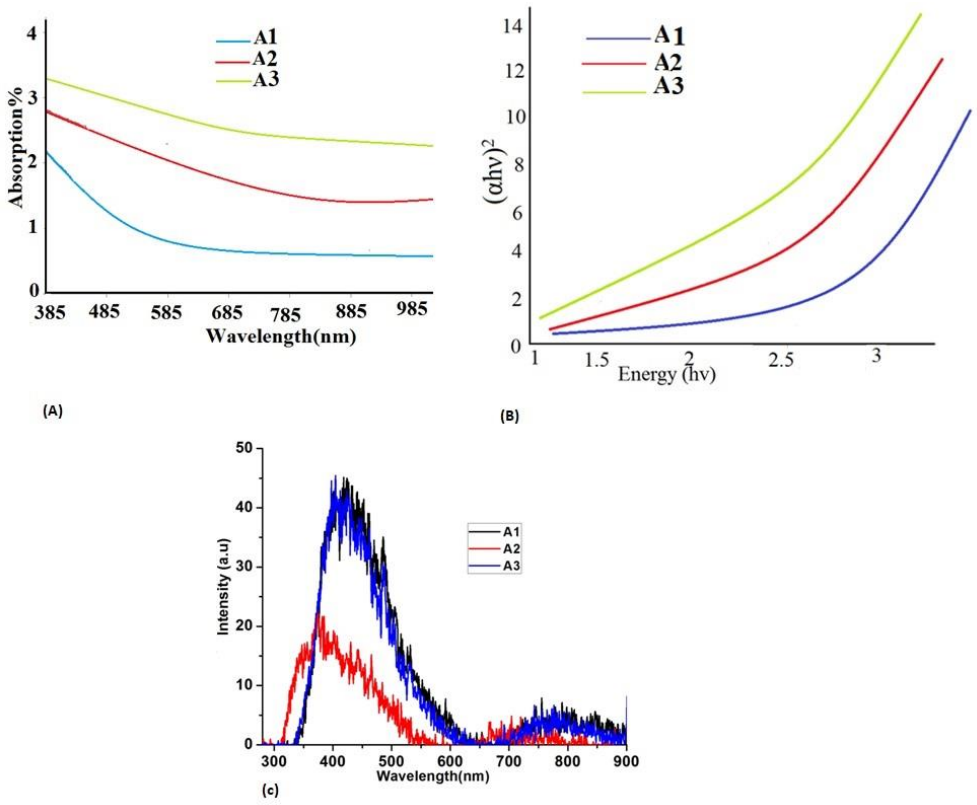


**Fig. 6. (a) UV-vis spectra (b) $(ahv)^2$ vs hν plots (c) Luminescence peaks of PS/$SnO_2$ samples (Samples A1, A2 and A3)**

## EFFECT OF CATALYST LOADING ON PHOTOCATALYTIC DEGRADATION OF DYES

Effect of catalysts loading on photocatalytic degradation of Indigo carmine dyes were studied with three different concentrations of nano composite samples : A1-1g PS $SnO_2$, A2-2g PS $SnO_2$, A3-5g PS $SnO_2$. under light from a 40 Watt LED bulbs in the photocatalytic chamber at room temperature. The mechanism of dye degradation is as follows:

Ground state dye molecules absorb radiation and get promoted to singlet excited state from which it will undergo intersystem crossover to triplet state. Valence band electrons in tin oxide will absorb radiation and get promoted to conduction band thus generating hole. The valence electron will react with the dissolved oxygen molecule in the solution to generate radical. Radicals react with dye molecule to generate dye superoxide ion thus degrading into carbon dioxide and water molecules. On the other hand, holes present in the valence band will react with hydroxyl ions to generate hydroxyl-free radical which attacks dye to generate degraded products.

Steps of equations-

$$PS - SnO_2 + PS - SnO_2 hv \quad \rightarrow \quad (e^- + h^+)$$

$$H_2O + h^+ \rightarrow OH^* + H^+$$

$$O_2 + e^- \rightarrow O_2^-$$

$$O_2^- + H_2O \rightarrow H_2O_2$$

$$H_2O_2 \rightarrow 2OH^*$$

$$OH^* + \text{Indigo carmine Dye} \rightarrow \text{degraded product}$$

The absorbance measurements were carried out at 600nm using UV-Vis spectrophotometer (Perkin Elmer Lambda-25) shown in Fig 7(a) after 30min. A decrease in absorbance value of indigo carmine dye solution was observed with various concentrations. Sharp decrease in absorption is observed that indicates how efficiently the PS nanocomposites catalyze the indigo dye. Low absorption peak for higher dose indicates the less residual presence of dye conversion of the dye into degrade product $H_2O$ and $CO_2$. Fig. 7(b) shows degradation of indigo carmine dye concentration with different samples after 30 min exposure to the light.

Percentage degradation is shown through histogram in Fig. 7(c). Sample A3 of higher dose is shown 99% removal of dye form the solution, indicates exceptionally good potential for developed as photocatalytic material for removal of Indigo carmine dye.

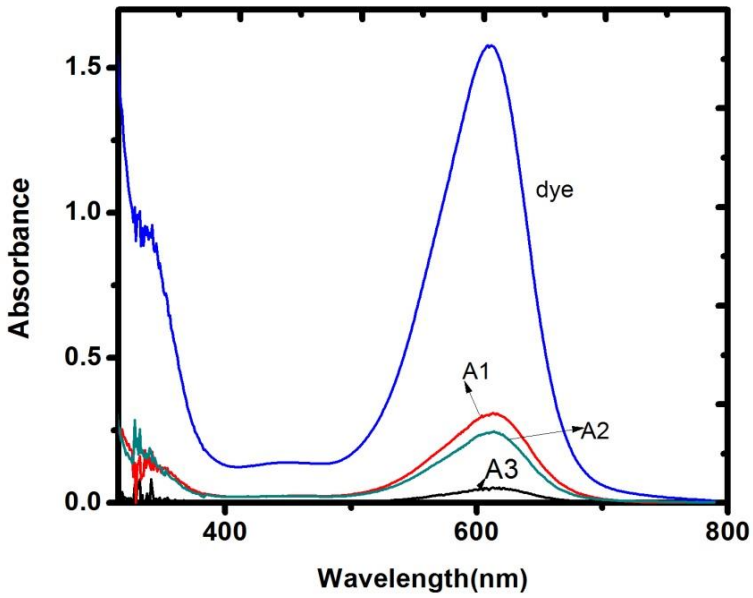

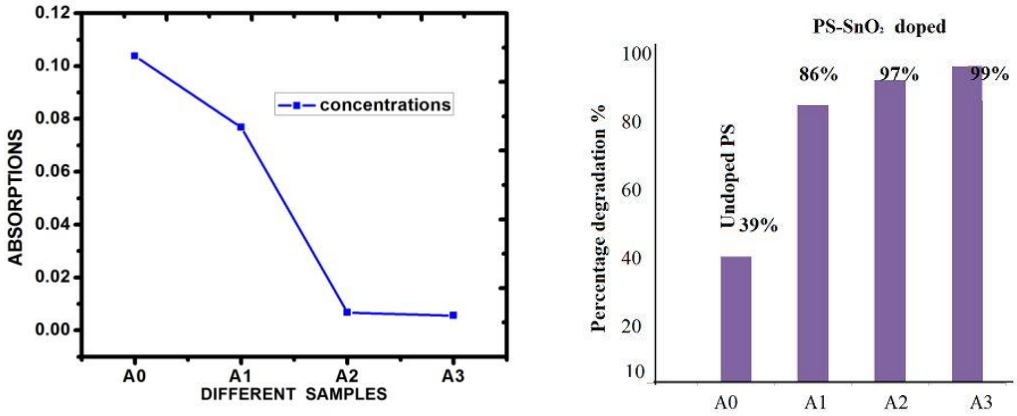


**Fig.7. (a) Absorption versus Wavelength curves for various samples A0, A1, A2 and A3 showing degradation of indigo carmine dye concentration with different samples after 30 min exposing of light on it (b) Absorbance vs samples and (c). histogram of degradation of dye [Sample undoped PS, A0- undoped; A1-1g PS $SnO_2$ , A2-2g PS $SnO_2$ and A3-5g PS $SnO_2$**

**Conclusions: -**

$SnO_2$: PS Nanocomposites were synthesized using thermocol packing waste by chemical route. X ray diffractograms shows crystalline behavior of $SnO_2$ embedded PS nanocomposites. Polystyrene shows crystalline behavior on higher concentration of $SnO_2$ nanoparticles. Crystalline behavior of PS-$SnO_2$ nanocomposites increases. Composites are amorphous on small concentration of $SnO_2$ nanoparticles. AFM shows spherical structures hollow vertical growth make the composites suitable for sensing applications. The size of spherical structures increases on increasing the amount of $SnO_2$ nanoparticles in PS. There is regular arrangement of nanoparticles shows good crystallite in composites. A regular chain is also observed. Samples are transparent in visible region and give band gap of around 3.0 eV. Strong photoluminescence peak also make them suitable for optoelectronic applications. In photocatalytic study results show that, Indigo blue can be efficiently degraded by heterogeneous photocatalysis process in aqueous suspension of $SnO_2$: PS Nanocomposites SnO2 as photocatalyst under UV Vis irradiation. The degradation of Indigo dye was found to dependent on dose concentration. Under the above optimum conditions, 99% Indigo dye degradation was achieved within 30 minutes make it suitable for development of photocatalytic for indigo carmine dye.

**Acknowledgement:**

The authors are thankful to MP Council of science and technology (MPCST) for providing research grant. Authors are also thankful to UGC-DAE consortium for scientific research, Indore India for providing AFM facilities (Mr. Mohan Gangrade) and Jiwaji university, Gwalior for XRD facilities and PC Ray research centre, ITM University Gwalior for providing optical and Photoluminescence facilities.

*Declarations*

**Funding** : The work was funded by MP Council of Science and Technology MP, India

**Conflicts of interest/Competing interests:** On behalf of all authors, the corresponding author states that there is no conflict of interest.

**References**

1. Gamze Dogdu Okcu , Tugba Tunacan, Emre Dikmen And Bolu Abant Izzet , Environmental Research & Technology, Vol. 2(2019),63-72.Doi:Https://Doi.Org/10.35208/Ert.457739.
2. Kirana D Veeranna, Madhu T Lakshamaiah, And Ramesh T Naraya , International Journal Of Photochemistry Volume 2014, 530570, 6 http://Dx.Doi.Org/10.1155/2014/530570.
3. Surya Lubis , Sheilatina , Dina Wardani Sitompul ,Mater. Sci. Eng. Volume2019, 509 012142. Doi:10.1088/1757-899X/509/1/012142
4. Bekri-Abbes, I., Bayoudh, S., Baklouti, M. J. Polym. Environ. 14(2006), 249–256.
5. Achilias, D.S., Kanellopoulou, I., Megalokonomos, P., Antonakou, E., Lappas, Mater. Eng. 292 (2007) 923–934.
6. Maharana, T., Negi, Y.S., Mohanty, B, Polym.-Plas Technol. 46 (2007) 729–736.
7. García, M.T., Gracia, I., Duque, G., Lucas, Ad, Rodríguez, J.F, Waste Management 29 (2009) 1814–1818.
8. Chae, D. W.; Kim, B. C. Polym Adv Technol, Journal of NanomaterialsVolume16 (2012) 846-850
9. Ma, C. C. M.; Chen, Y. J.; Kuan, H. C. J Appl Polym Sci, 100 (2006) 508-515.
10. Zhong, W.; Liu, P.; Shi, H. G., Xue, D. S. Express Polym Lett 4, (2010) 183–187.com
11. G. Nenna, A. De Girolamo Del Mauro, E. Massera, A. Bruno, T. Fasolino, and C. Minarini , 7 (2012) 319398.
12. Ali, T.; Venkataraman, A. Int J Adv Eng Technol, 7 (2014) 122-126. ISSN(e): 2311-763X ISSN(p): 2312-0991.
13. Qianqian Ding, Lifeng Hang and LiMa, Materials Letters,Volume 125 (2014), 120-123.
14. Kassaee, M.Z., Motamedi, E., Majdi, M., Chem. Eng. J. 172 (2011) 540–549.
15. Polystyrene : synthesis, characteristics, and applications / editor, Cole Lynwood, http://www.novapublishers.com. TP1180.S7P665 2014,668.4'233--dc23.
16. Ruziwa, D., Chaukura, N., Gwenzi, W., Pumure, I, J. Environ. Chem. Eng. 3(2015) 2528–2537.
17. Mashael Nasser ,Alshabanat and Murefah M. AL-Anazy. Journal of Chemistry, 8(2018), 965-1850.
18. P. G. Harrison and M. J. Willet Nature, (1988), 332, 337.
19. Neha Bhardwaj, Sini Kuriakose, S. Mohapatra , Journal of Alloys and Compounds 592 (2014 ) 238–243.
20. S. Ferrere, A. Zaban and B. A. Gregg,. J. Phys. Chem. B,101 (1997) 4490..
21. J. Zhu, Z. Lu, S. T. Aruna, D. Aurbach and A. Gedanken, Chem. Mater, 12 (2000) 2557.

22. Y. Wang, X. Jiang and Y. Xia, J. Am. Chem. Soc., 125 (2003) 16176.
23. G. Xi and J. Ye, Inorg. Chem., 49 (2010) 2302. https://doi.org/10.1021/ic902131a
24. S. Sain, A. Kar, A. Patra and S. K. Pradhan, , , Cryst Eng Comm, 16( 2014) 1079.
25. Z. Liu, D. Zhang, S. Han, C. Li, T. Tang, W. Jin, X. Liu and C. Zhou, Adv. Mater,15(2003) 1754.
26. Y C Goswami, Vijay Kumar and P Rajaram , V. Ganesan, Mohammad Azad Malik, Paul O'Brien, Journal of Materials Science Materials in Electronics 69(2014) 617-624
27. Soumen Das, Soumitra Kar, and Subhadra Chaudhuri, Journal of Applied Physics , 99 (2006) 114303.
28. Y C Goswami, Vijay Kumar and P Rajaram,Materials Letters (Elsevier) 128 (2014) 425–428.
29. F. Javier Yusta, Michael L. Hitchman and Sarkis H. Shamlian.,*J. Mater. Chem.*, 7 (1997) 1421-1427.
30. Geovania C. de Assis, Euzébio Skovroinski,Valderi D. Leite,Marcelo O. Rodrigues,André Galembeck,Mary C.F. Alves, Julian Eastoe, and Rodrigo J. de Oliveira, , ACS Appl. Mater. Interfaces 10 (2018) 8077−8085.
31. Yong-Qiang Liu,Ge-Bo Pan,Meng Zhang and Feng Li.. Materials Letters 92(,2013) 284–286.
32. B.D. Cullity & S.R. Stock, *Elements of X-Ray Diffraction*, 3rd Ed., Prentice-Hall Inc., 2001, p 167-171, ISBN 0-201-61091-4.

# Figures

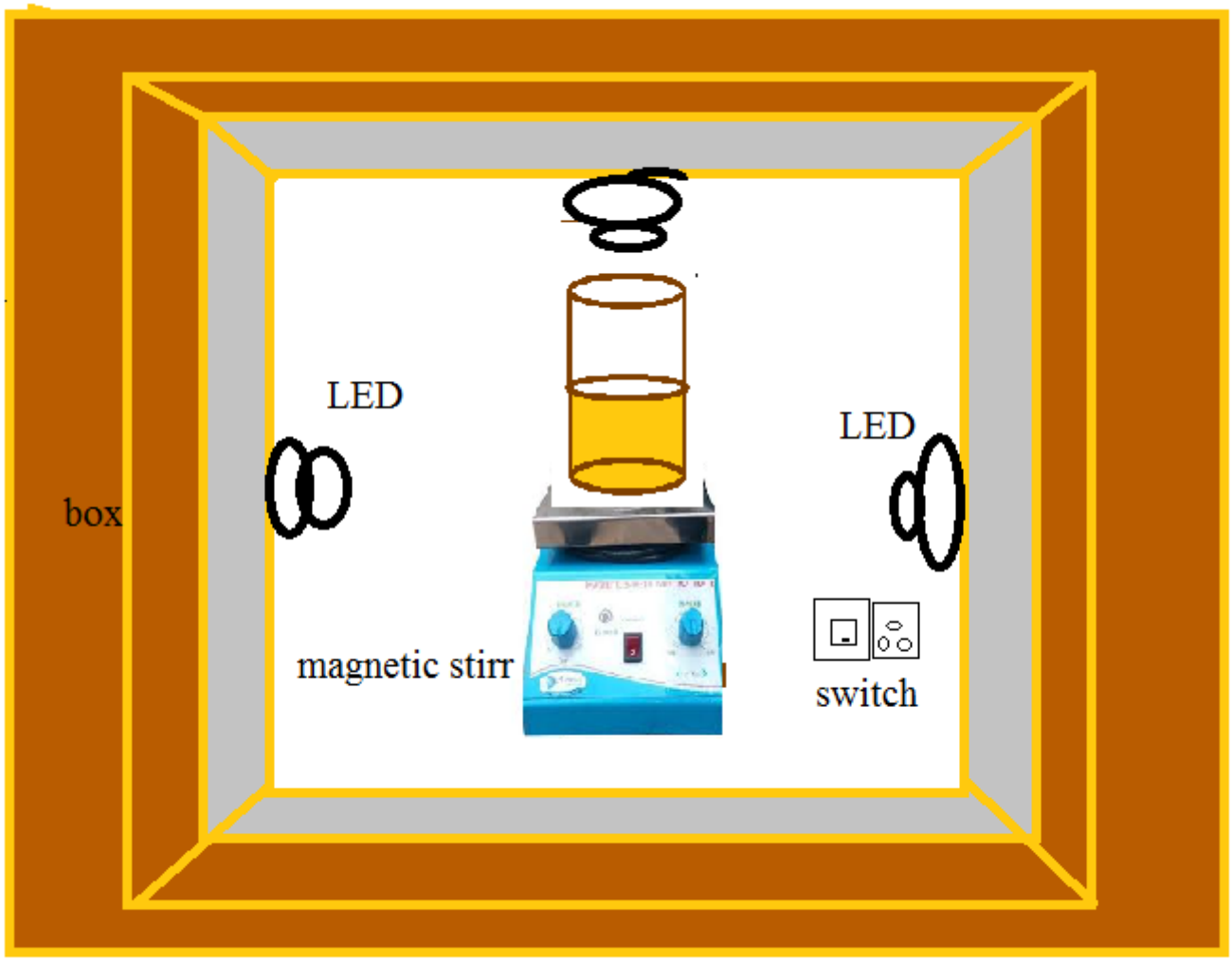


**Figure 1**

schematic diagram of Photocatalytic reactor Photocatalytic activity

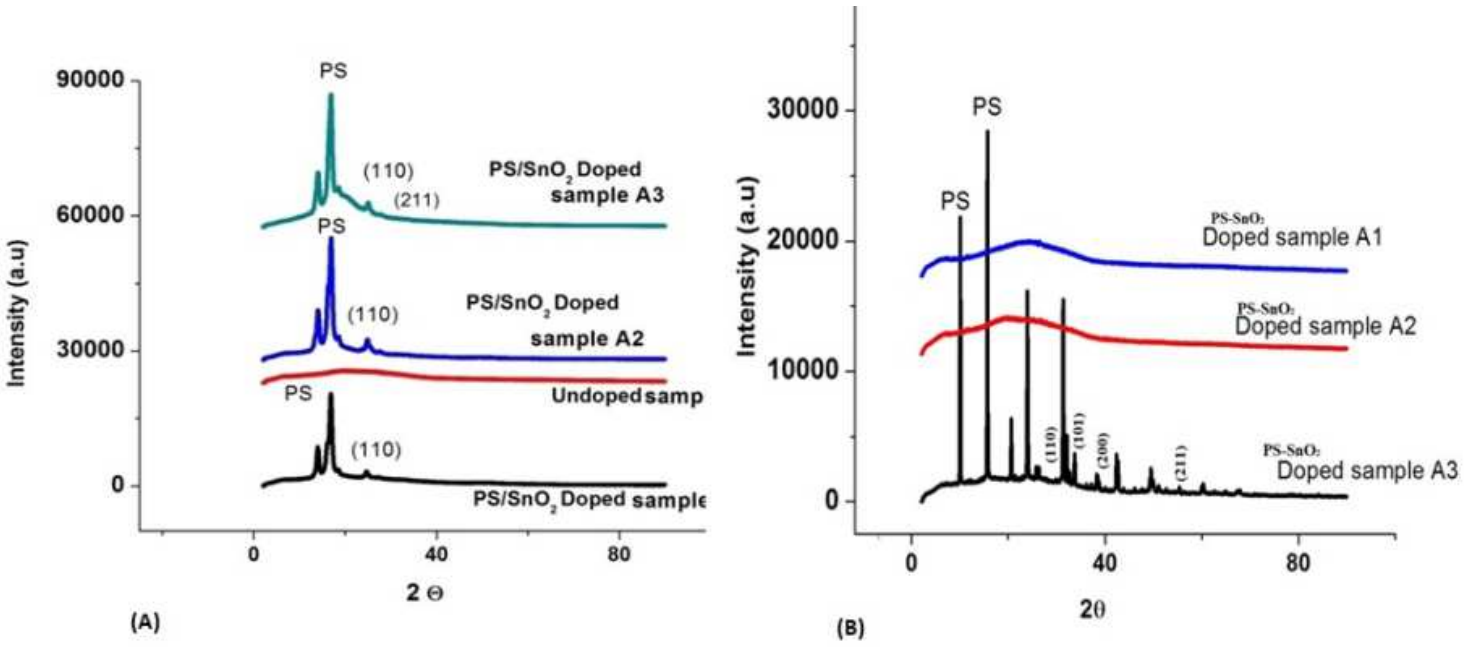


## Figure 2

X ray diffractograms for (a) flexible self sustained films (b) on glass substrate with various SnO2 concentrations (A) Undoped A0 (B) A1:1g PS/ SnO2 (C)A2:3g PS/SnO2 (D) A3: 5g PS/ SnO2.

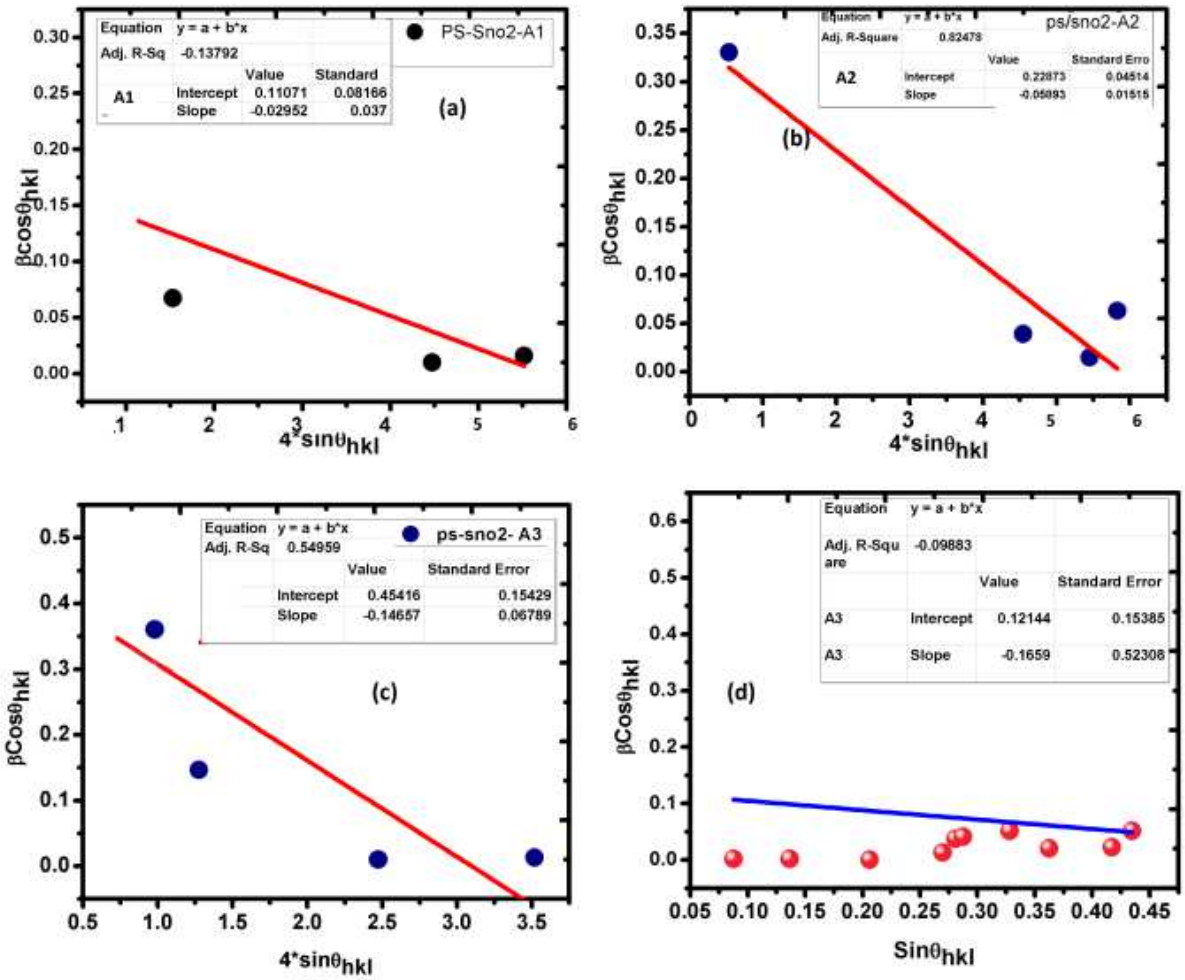


## Figure 3

W H plots of film on glass substrate (a), (b), (c). and in fig (d) WH plot of flexible film sample A3 with slope and intercept.

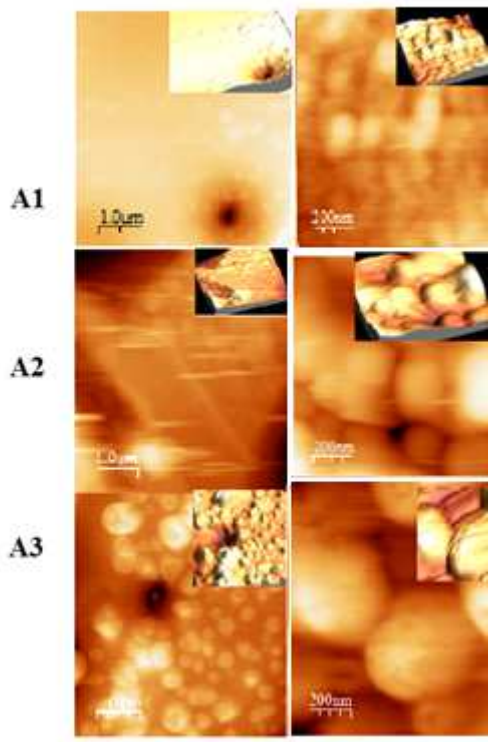


**Figure 4**

Atomic force micrograph of SnO2/PS Nanocomposites 2D view and 3D view of samples (a) A1-PS/ SnO2 (b) A2-PS/ SnO2 (c) A3-PS/ SnO2.

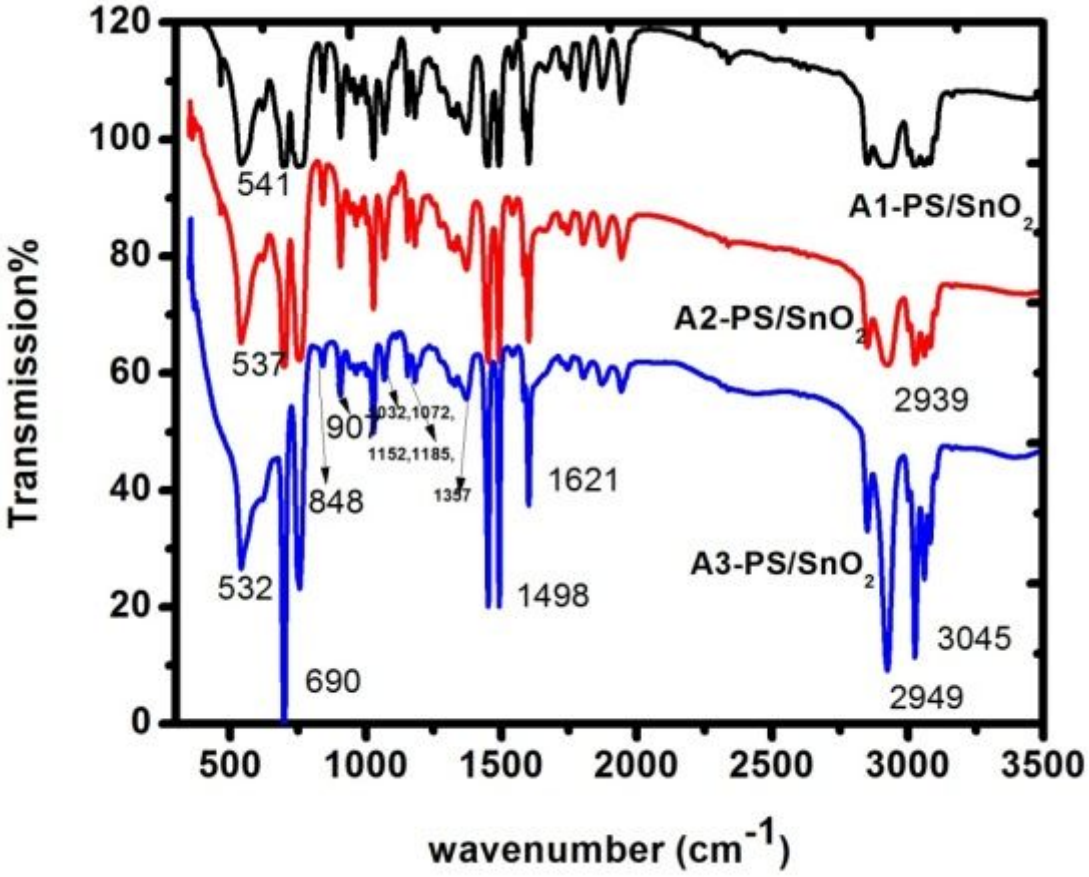


**Figure 5**

FTIR spectra of (A) Undoped A0 (B) A1:1g PS/ Sno2 (C) A2:3g PS/Sno2 (D) A3: 5g PS/ SnO2.

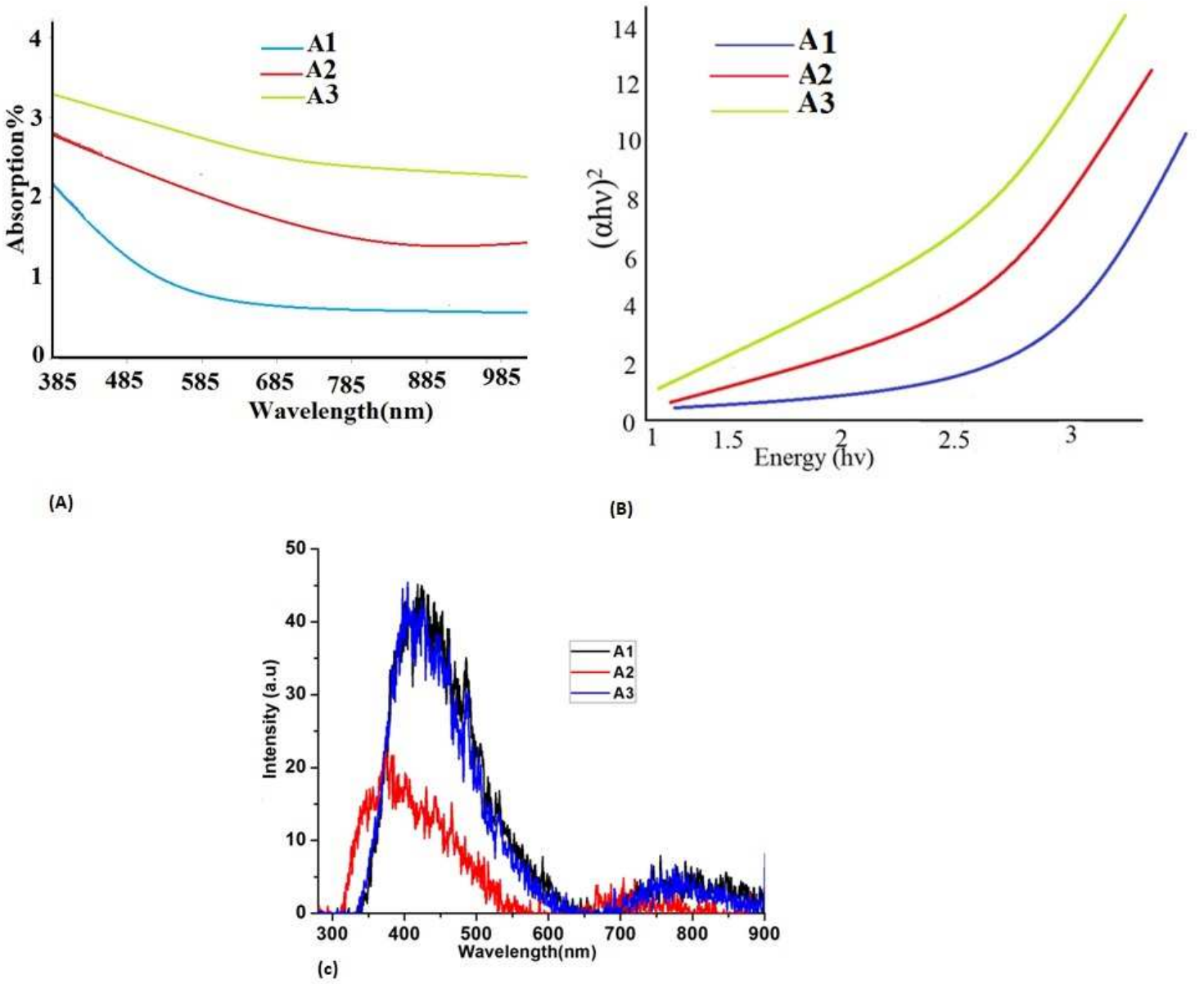


## Figure 6

(a) UV-vis spectra (b) (ahv)2 vs h plots (c) Luminescence peaks of PS/SnO2 samples (Samples A1, A2 and A3)

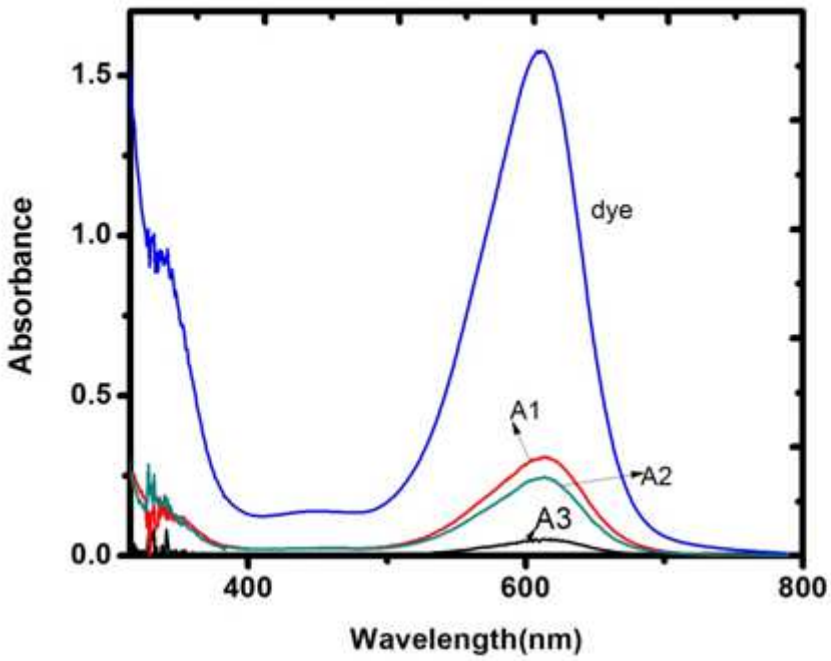


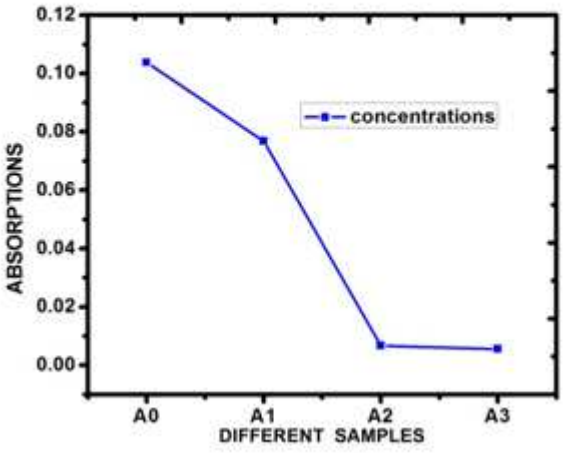


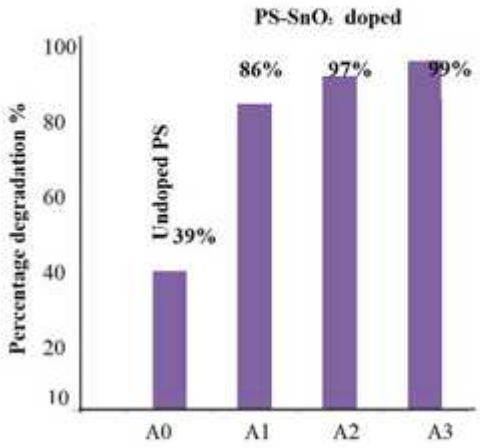


## Figure 7

(a) Absorption versus Wavelength curves for various samples A0, A1, A2 and A3 showing degradation of indigo carmine dye concentration with different samples after 30 min exposing of light on it (b) Absorbance vs samples and (c). histogram of degradation of dye [Sample undoped PS, A0- undoped; A1- 1g PS SnO2 , A2-2g PS SnO2 and A3-5g PS SnO2